RSC Advances

ROYAL SOCIETY OF CHEMISTRY

www.rsc.org/advances

Graphical Abstract for

Antibacterial Properties and Mechanisms of Toxicity of Sonochemically Grown ZnO Nanorods

Tugba O. Okyay,[a] Rukayya K. Bala,[b] Hang N. Nguyen,[a] Ramazan Atalay, [b] Yavuz Bayam*[b] and Debora F. Rodrigues*[a]

[a] *Department of Civil and Environmental Engineering. University of Houston, Houston, TX-77004, USA. Fax: 713-743-4260; Tel: 713-743-1495; E-mail: dfrigirodrigues@uh.edu*

[b] *Department of Electrical and Electronics Engineering. Gediz University,35660 Izmir, Turkey. Fax: +90(232)355 0046; Tel:+90(232)355 0000; E-mail: yavuz.bayam@gediz.edu.tr*

ZnO nanorods produced sonochemically prevented microbial growth, biofilm formation and were non-toxic to mammalian cells.

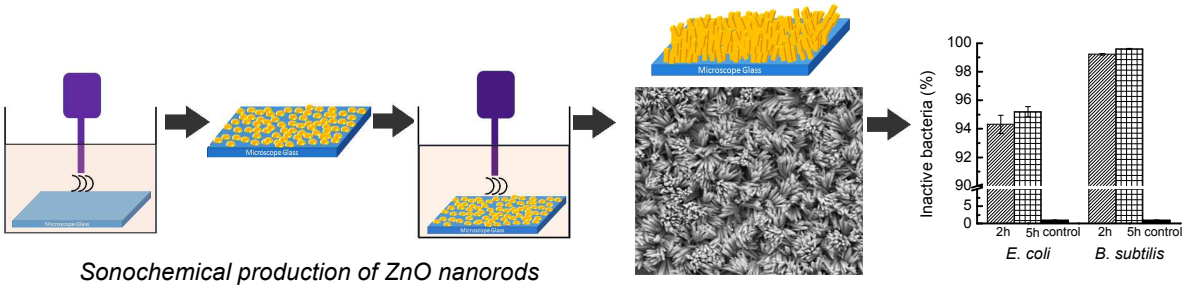

Sonochemical production of ZnO nanorods

Cite this: DOI: 10.1039/c0xx00000x

www.rsc.org/xxxxxx

ARTICLE TYPE

Antibacterial Properties and Mechanisms of Toxicity of Sonochemically Grown ZnO Nanorods

Tugba O. Okyay,[a] Rukayya K. Bala,[b] Hang N. Nguyen,[a] Ramazan Atalay,[b] Yavuz Bayam*[b] and Debora F. Rodrigues*[a]

Received (in XXX, XXX) Xth XXXXXXXXX 20XX, Accepted Xth XXXXXXXXX 20XX
DOI: 10.1039/b000000x

In this study, we present a simple, fast and cost-effective sonochemical growth method for the synthesis of zinc oxide (ZnO) nanorods. ZnO nanorods were grown on glass substrates at room temperature without the addition of surfactants. The successful coating of substrates with ZnO nanorods were demonstrated by Raman spectroscopy, X-ray photoelectron spectroscopy (XPS), scanning electron microscopy (SEM), and energy dispersive X-ray spectroscopy (EDS). Antimicrobial properties of ZnO nanorods against the planktonic *Bacillus subtilis* and *Escherichia coli* and their respective biofilms were investigated. The cytotoxicity of ZnO nanorods were evaluated using the NIH 3T3 mammalian fibroblast cell line. Moreover, to understand the possible mechanisms of ZnO nanorod toxicity, glutathione oxidation, superoxide production, and release of Zn^{2+} ions by the ZnO nanorods were determined, and the LIVE/DEAD assay was employed to investigate cell membrane damage. The results showed that sonochemically grown ZnO nanorods exhibited significant antimicrobial effects to both bacteria and prevented biofilm formation. ZnO nanorods did not present any significant toxicity to fibroblast cells. The main anti-microbial mechanisms of ZnO nanorods were determined to be H_2O_2 production and cell membrane disruption.

Keywords: Zinc oxide, sonochemistry, nanorods, human cytotoxicity, antibacterial, biofilms

1. Introduction

Materials at the nanometer scale in the size range of 1-100 nm possess extraordinary physical, chemical and biological properties that are far different from those in the bulk form. These properties give nanomaterials a great potential to revolutionize the fields of electronics, materials science and medicine. Since the size of the nanomaterials and biomolecules differ by only one order of magnitude, they are able to interact with each other in complex biological systems. This unique property of nanomaterials opens a new window for novel biomedical applications including prevention, diagnosis and treatment of many diseases.[1]

In the past few years, ZnO nanomaterials have been attracting a significant amount of attention due to its wide band gap (3.37 eV), large exciton binding energy (60 meV), transparency and high luminescence at room temperature that allow application in different engineering, medical, and materials science fields. For instance, the possibility of growing ZnO nanostructures on surfaces has been showing great potential for applications in the optoelectronic and biomedical industry, such as photo detectors and drug delivery for cancer cell therapy.[2, 3] Moreover, the high-sensing capability and high electron mobility of ZnO nanostructures have been widely explored for various applications, such as biosensors for intracellular measurements as well as gas, pH and temperature sensors.[4-7]

Recent studies have shown that ZnO is known to exhibit antimicrobial properties toward both Gram-negative and Gram-positive bacteria, as well as bacterial spores, which are resistant to high temperatures and pressures.[8-10] Due to its antimicrobial properties, ZnO nanoparticles have great potential for use in the manufacture of anti-microbial cotton fabrics and food packaging, as well as medical devices to prevent antimicrobial infection.[11, 12] For example, a recent study reported that the use of ZnO nanorods on paper prevented its deterioration and suggested that these nanomaterials could be used to produce facemasks, tissues, wallpapers and writing papers with antimicrobial properties.[13] This study, yet of great relevance, has not, however, used a systematic investigation to understand the anti-microbial mechanisms of ZnO nanorods on surfaces and their potential human toxicity for application in medical devices.

Other studies involving ZnO nanorods synthesis demonstrated that it was possible to synthesize well-aligned, single crystalline 0-D and 1-D nanostructures of ZnO with different morphologies and diameters for different applications. These studies used various techniques including both top-down approaches by wet etching and bottom-up such as chemical vapor deposition (CVD), vapor liquid solid (VLS), metal-organic chemical vapor deposition (MOCVD), pulse laser deposition (PLD) and

hydrothermal techniques.[14-19] More recently, the sonochemical growth method of metal oxides, such as ZnO nanostructures, has received a lot of interest from different researchers because it has been shown to be a suitable technique to coat any substrate that is stable in alcohol or in aqueous solutions at room temperature. Furthermore, sonochemistry has been showing to be the most suitable method for substrates that are not resistant to high temperatures.[20, 21]

In this study, ZnO nanorods were grown by a cost-efficient sonochemical growth method at room temperature using zinc nitrate tetrahydrate and hexamethylenetetramine (HMT). The successful synthesis and coating of glass surfaces with ZnO nanorods were determined by structural, elemental and surface morphological analyzes. Additionally, the anti-microbial property of these coatings against bacteria was also probed to determine whether this new method produces anti-microbial coatings. The mechanisms of anti-microbial properties of the nanorods were investigated using the Ellman's, XTT (2,3-bis-(2-methoxy-4-nitro-5-sulfophenyl)-2H-tetrazolium-5-carboxanilide), the Zn^{2+} release from the ZnO nanorods and LIVE/DEAD assays. The safety of the nanomaterial was also determined using NIH 3T3 mammalian fibroblast cells.

2. Experimental

2.1. Preparation and characterization of the ZnO nanorods

The ZnO nanorods were grown on glass substrates by employing a sonochemical growth method. The glass substrates were first cleaned using a solution of isopropyl alcohol, acetone and distilled water, respectively, in an ultrasonic bath for 20 minutes, then dried using nitrogen gas. Before the growth of ZnO nanorods, a seed layer of ZnO nanoparticles was deposited on the glass substrates to serve as nucleation sites and to guide the orientation and morphology of the ZnO nanorods.[22] Deposition of the seed layer was performed using zinc acetate dehydrate ($C_4H_6Zn{\cdot}2H_2O$). A solution of 0.005 M zinc acetate dihydrate in isopropyl alcohol was prepared at room temperature. Clean glass substrate was then immersed into the solution and sonicated for 30 min at 50% of the maximum amplitude of the 400 W ultrasonic probe working at 24 kHz. After deposition of the seed layer, the ZnO nanorods were grown using an aqueous solution of 0.04 M zinc nitrate tetrahydrate ($Zn(NO_3)_2{\cdot}4H_2O$) and 0.04 M hexamethylenetetramine ($(CH_2)_6N_4$). Equal volumes of the solutions were mixed with a magnetic stirrer at 750 rpm for 5 min. The substrate was then immersed in the solution and sonicated for 60 min at 400W amplitude with a 24 kHz ultrasonic probe. **Fig. 1** shows the steps involved in the sonochemical synthesis of ZnO nanorods.

The Raman scattering characterization was performed by a confocal Raman spectroscopy with an excitation wavelength of 488 nm (2.54 eV) at room temperature. The chemical composition of ZnO nanorods was determined using an energy dispersive X-ray spectroscopy (EDS) module attached to the scanning electron microscope (SEM) (FEI Quanta 250 FEG). X-ray photoelectron spectroscopy (XPS) characterization was performed using PHI 5700, which was equipped with an electronic supplementary material for chemical communication with the monochromatic Al KαX-ray source (hν = 1.4867 keV) incident at 90° relative to the axis of a hemispherical energy analyzer.

Suspensions of sonochemically grown ZnO nanorods were also prepared. For this aim, the same ZnO nanorods synthesis protocol was followed, but no seed layer step was included. After getting the suspension of ZnO nanorods, a lyophilisation step was employed at -80°C to obtain powder nanorods. For all experiments with the ZnO nanorods in solution, the powder ZnO nanorods were weighed, suspended in water, and homogenously dispersed using a tip sonicator for 15 min prior to use. These ZnO nanorod solutions were used in the glutathione oxidation and XTT reduction assays (see SI †).

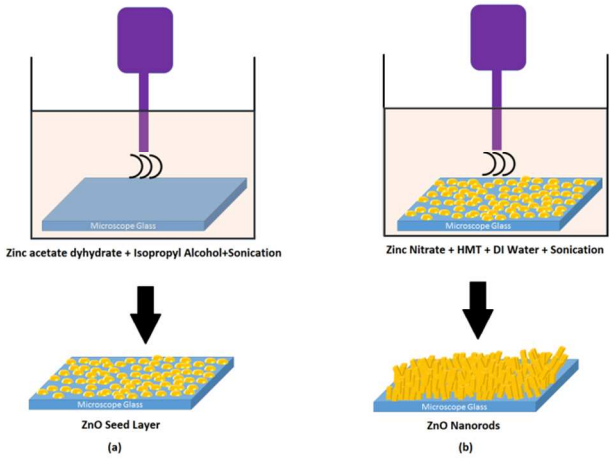

Fig. 1 Flow chart of sonochemical synthesis of a) ZnO seed layer b) ZnO nanorods on the glass slides.

2.2. Microorganisms and growth conditions

E. coli MG 1655 and *B. subtilis* 102 were used for the antimicrobial investigations. Both microorganisms were grown in tryptic soy broth (TSB) (Oxoid) at 37°C under 150 rpm shaking for 16 h prior to each experiment. After cultivation, cells were harvested by centrifugation at 10,000 rpm for 10 min, and washed trice with phosphate buffered saline solution (PBS, 0.01M, pH=7.4) (Fisher Scientific) to eliminate the culture media components. Cells were resuspended in PBS to an optical density (OD) of 0.5 at 600 nm, which corresponds to 10^7 colony forming units per millilitre (CFU/mL).[23]

2.3. Toxicity of ZnO nanorods to bacterial cells

Pieces of glass slides (1 cm x 1 cm) with sonochemically grown ZnO nanorods were used in all toxicity assays. Bare slides of similar sizes were used as negative controls in all experiments, unless indicated otherwise. All experiments were performed in triplicate. In order to understand the effect of time on the anti-microbial properties of the coated surfaces, cells were exposed to nanorods for 2 h and 5 h.

2.3.1. Short term exposure asssays

Aliquots of 2 mL of bacterial suspension at 0.5 $OD_{600\ nm}$ in PBS were incubated at 37°C for 2 h and 5 h without shaking with a piece of glass coated or not with ZnO nanorods. After 2 h and 5 h exposure times, the glass pieces were removed using sterile tweezers and their uncoated sides were carefully cleaned to prevent contamination by bacteria that were not exposed to

nanomaterials. The control slides also had one of their sides cleaned prior to analyses. The glass pieces were then placed in a sterile Petri dish for washing with 1 mL of sterile PBS solution in a Petri dish. For washing, a bath sonicator was used for 1 min. The effective cell removal by the slide wash procedure was determined by microscopy. The washing solution was diluted serially in PBS (10^{-7}, 10^{-6}, 10^{-5}, 10^{-4}, and 10^{-3}). The dilutions were plated in tryptic soy agar (TSA) plates and incubated overnight at 37°C. The live bacteria after exposure to the nanomaterial was quantified as CFU mL^{-1} in each plate.[24] The assays were performed in triplicates in three different days to ensure reproducibility of the results. The results of the experiments were averaged out and their respective standard deviations were calculated. The percent toxicity was expressed as the percent of the ratio of the dead cells exposed to the ZnO nanorods to the control cells as described by Mejias *et al*.[23]

2.3.2. Long term exposure

A 12-well plate containing glass pieces with or without ZnO nanorods was inoculated with 10% cell solutions in 4 mL of TSB. The well-plates were incubated at 37°C without shaking for 48 h and at the end of the incubation period, the glass pieces were removed with sterile tweezers. The biofilms on the surfaces were fixed, stained, and analyzed with SEM as previously described.[25]

2.4. Cytotoxicity of ZnO nanorods to mammalian cells

Suspensions of sonochemically grown ZnO nanorods with concentrations between 0.1 to 40 ppm were investigated for their cytotoxicity against the NIH 3T3 mammalian fibroblast cell line using the CellTiter 96® AQ_{ueous} One Solution Cell Proliferation Assay (Promega). The fibroblast cells were obtained from MD Anderson Cancer Center, Houston, Texas. All incubations with fibroblasts were completed at 37°C in a 5% CO_2 humidified incubator (NuAire), unless indicated otherwise. All assays were performed in triplicates and repeated at least three times.

NIH 3T3 cells (cells of passages 2 and 9) were grown for 48 h in Dulbecco′s Modified Eagle′s Medium (DMEM) (Catalog #D6546, Sigma Aldrich) with additional L-glutamine and fetal bovine serum to a final 10% concentration. Next, the spent medium was aspirated, and 4 mL of TrypLE was added and incubated for 10 min. Afterwards, centrifugation was achieved at 300 *g* for 2 min and the cell solution was prepared by suspending the cells in fresh DMEM and quantifying with a hemocytometer to have a cellular density of 3×10^4 cells per 100 µL. A sterile 96-well plate (Falcon) was prepared by placing 100 µL of cell solution into each well and incubating the plate for 24 h to achieve optimum cell growth. After 24 h, the spent medium was aspirated from each well, and all wells were gently rinsed three times with sterile PBS. The wells were then, ready for the cytotoxicity assay, and 100 µL of fresh media and 100 µL of ZnO nanorods solution were added to each well. In order to confirm the specific chemical interference of ZnO nanorods solution, a control was prepared as follows; 100 µL of nanorods solution and 100 µL of media were mixed in wells with no cells. To eliminate the background effect of the assay, the absorbance of this control was subtracted from the absorbance of the samples. Furthermore, PBS with no ZnO nanorod solution in the wells containing fibroblast cells was used as negative control, while the positive control was PBS containing 0.02% of benzalkonium chloride (BAC). The 96-well plate was gently mixed once and incubated for 12 h. After incubation, the growth medium was aspirated from the wells, and the wells were rinsed with PBS three times. Next, the detection reagent of the assay, MTS [3-(4,5-dimethylthiazol-2-yl)-5-(3-carboxymethoxyphenyl)-2-(4-sulfophenyl)-2H-tetrazolium], and fresh DMEM were added to all wells (with and without cells) with a ratio of 1:5, respectively, and the plate was incubated for another 3 h. The quantity of formazan product formed, as measured by the absorbance at 490 nm, is directly proportional to the number of living cells in culture; hence the absorbance at 490 nm was recorded using a microplate reader (FLUOstar Omega, BMG Labtech). The results were expressed in terms of percentage of the living cells compared to the negative control and the calculation was done as follows:

Cell viability (%) = [$(A_{sample} - A_{background})$ / $(A_{negative\ control} - A_{background})$] x 100

2.5. Toxicity mechanisms

2.5.1. GSH oxidation assay

The production of reactive oxygen species (ROS) are known to cause oxidative stress in cells and have been reported in previous studies to explain the possible mechanisms of toxicity of diverse nanomaterials.[26] Oxidation of glutathione (γ-L-glutamyl-L-cysteinyl-glycine, GSH), a thiol containing polypeptide present in prokaryotic and eukaryotic cells and known to protect the cells from stress caused by ROS, is commonly used as an indirect method to quantify the ROS production in aqueous solutions with the presence of nanomaterials.[27] The ROS production due to the sonochemically grown ZnO nanorods on glass substrates was investigated according to the Ellman's assay.[28] ZnO nanorod solutions with different concentrations (1-200 ppm) were incubated with the GSH solution in a bicarbonate buffer using a 12-well plate. The plate was incubated at room temperature for 2 h in the dark to prevent any photochemical reaction. After 2 h, the Ellman's reagent [5,5-dithio-bis-(2-nitrobenzoic acid) (DTNB)] was added into each well to react with the GSH. The resultant yellow solutions were filtered using 0.22 µm syringe filters (VWR) to remove any particles from the solutions. A volume of 200 µL of the solution was placed in a 96-well plate to read the absorbance at 412 nm with the Synergy MIX Microtiter plate reader (BioTek, USA). The negative control did not contain any ZnO nanorods, whereas the positive control contained 30% of H_2O_2 for the GSH oxidation. The results were expressed in terms of percentage of the GSH loss and the calculation was done as follows:

GSH loss (%) = [$(A_{negative\ control} - A_{sample})$ / $A_{negative\ control}$] x 100

2.5.2. LIVE/DEAD assay

To understand the toxicity mechanism of sonochemically grown ZnO nanorods and to see the cell membrane disruption, LIVE/DEAD Baclight bacterial viability kit (Invitrogen) was used to stain the cells on the glass slides containing ZnO nanorods as described earlier.[23] The kit has two nucleic acid dyes: SYTO9 and propidium iodide (PI). SYTO9 stains all cells on the glass slide in green, while PI stains only dead cells in red when there is cell membrane disruption. The fluorescent images were taken using BX 51 Olympus Fluorescent Microscope equipped with a DP72 digital camera under 100X objective and a

fluorescinisothiocyanate (FITC) filter.

3. Results and discussion

Homogeneous surface coatings with ZnO nanorods were successfully synthesized by ultrasonic irradiation of zinc nitrate tetrahydrate and hexamethylenetetramine (HMT). Surface morphology characterization revealed the formation of well coated surfaces with rod-like structures. Elemental analysis also confirmed that the structures were made purely of Zn and O.

3.1. Raman spectroscopy results

The micro-crystalline structures of the sonochemically grown ZnO nanorods were investigated by Raman spectroscopy. ZnO has a hexagonal (wurtzite) crystal structure, which belongs to the C^4_{6v} point group symmetry with two formula units per primitive cell. $A_1 + 2E_2 + E_1$ are the Raman active optical phonon modes predicted by the group theory, among which A_1 and E_1 are the polar phonons, which can split into transverse optical (TO) and longitudinal optical (LO) modes. E_2 is the non-polar mode, which is composed of two modes frequency $E_2^{(high)}$ associated with the vibration of oxygen atoms and $E_2^{(low)}$ is associated with the vibration of Zn sub-lattice.[29, 30]

Fig. 2 shows the representative Raman spectra of ZnO nanorods grown on glass substrate using the excitation energy of 488 nm (2.54 eV). The Raman spectrum of ZnO nanorods exhibited six prominent peaks at 210, 446, 495, 654, 1350, and 1450 cm^{-1} in addition to the glass substrate related peaks. The Raman spectrum of ZnO nanorods was quite different than that of the bulk material due to multiphonon modes that occurs in nanorods and nanotubes. The modes at 210, 446, and 654 cm^{-1} are assigned to the second order acoustic mode (2TA), $E_2^{(high)}$, and the acoustic overtone, respectively, and are in agreement with previously reported values.[31] The $E_2^{(high)}$ mode exhibited a symmetric prominent Lorentzian line shape; thus, it is a good indication of good local ordering (or microscopic crystallinity) of ZnO layers. The mode observed at 495 cm^{-1} is assigned to be a A_1(LO) peak position, but the peak position was shifted to lower frequencies (red shifting) from that of the bulk ZnO value due to oxygen deficiency and/or increase in the lateral grain size of the structures.

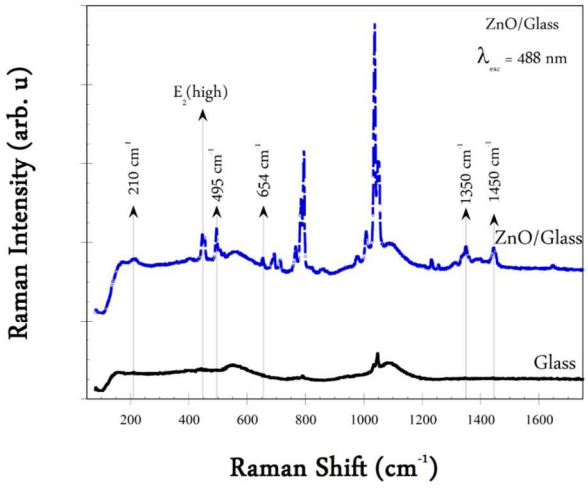

Fig. 2 Raman spectrum of sonochemically grown ZnO nanorods on glass substrate.

3.2. XPS results

The XPS measurements were performed to investigate the long-range ordering of the sonochemically grown ZnO nanostructures. The XPS survey spectrum exhibited well-resolved Zn and O elemental lines, which demonstrated successful synthesis of ZnO nanostructures. The inset of the **Fig. 3** shows detailed analysis of the Zn $2p_{3/2}$ photoelectron spectrum. The deconvolution of the Zn $2p_{3/2}$ photoelectron spectrum revealed three Zn peaks centered at 1021.6, 1022.7, and 1023.7 eV with full-width half maximum of (FWHM) 1.8, 1.28, and 0.77 eV, respectively. The main peak, centered at 1021.6 eV with peak width 1.8 eV, is in agreement with the literature value obtained from bulk Zn.[32] The two Zn $2p_{3/2}$ peaks (blue) shifted to 1022.7 and 1023.7 eV and may be attributed to (i) charge redistribution in process of chemical binding or (ii) different photoemissions of various Zn species (radicals).[33, 34]

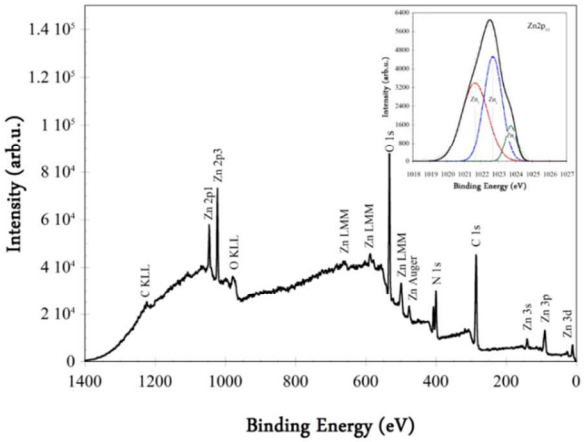

Fig. 3 Photoelectron spectrum of sonochemically grown ZnO nanostructures and inset shows deconvolution of Zn 2p3/2 photoelectron spectrum.

3.3. SEM and EDS results

The surface morphology and chemical composition analyses of the sonochemically grown ZnO nanostructures were investigated by SEM and EDS, respectively. As seen in **Fig. 4**, the SEM image showed that ZnO nanostructures covered completely and homogenously the glass substrate. The EDS spectrum indicated the presence of Zn, O, and Si atoms. The Zn and O are commonly found in ZnO nanorods. It is worth point out that the expected stoichiometric ratio for the ZnO nanorods was 1:1 between Zn and O atoms, instead, a ratio of 1:2 was observed in the EDS results. This unexpected ratio for the ZnO nanorod and the presence of Si atoms in the EDS spectrum can be explained by the fact that the coated substratum was a glass slide, which typically contains both Si and O atoms.[35]

3.4. Antimicrobial properties of ZnO nanorods

The anti-microbial properties of the ZnO nanorods were investigated over diverse time periods. The short-term microbial inactivation of Gram-positive and Gram-negative bacteria was investigated for 2 h and 5 h (**Fig. 5**). The long-term inactivation, to determine the ability of the ZnO nanorods to inhibit biofilm formation, was determined after 48 h (**Fig. 5**).

Cite this: DOI: 10.1039/c0xx00000x

www.rsc.org/xxxxxx

ARTICLE TYPE

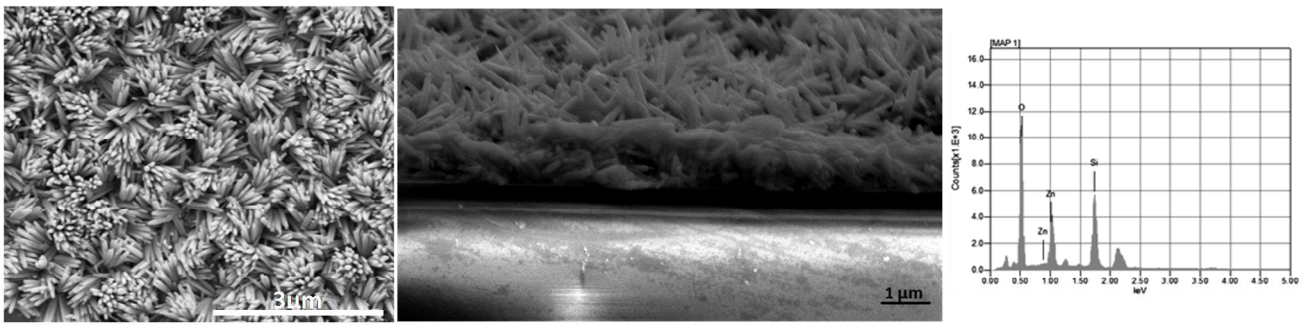

Fig. 4 Surface and cross-section SEM images of sonochemically grown ZnO nanorods on glass substrate and EDS spectrum of the coated slides.

In **Fig. 5**, the results show that bare glass slides (control) did not present any toxicity toward bacterial cells, whereas ZnO nanorods coated samples presented over 90% cell inactivation.

Among the different microorganisms investigated, *B. subtilis* was more sensitive to the presence of ZnO nanorods than *E. coli,* with 100% and 95% cell inactivation after 2 h of exposure to the ZnO nanorods, respectively. This result is similar to previous findings where nanostructures of ZnO were reported to exhibit higher toxicity toward Gram-positive than Gram-negative bacteria, which was attributed to structural differences in the cell wall.[36] As the incubation period increased, the toxicity of ZnO nanorods increased slightly, but was not statistically significant, as previously observed for other nanomaterials, such as graphene, graphene oxide, and carbon nanotubes.[28, 37, 38]

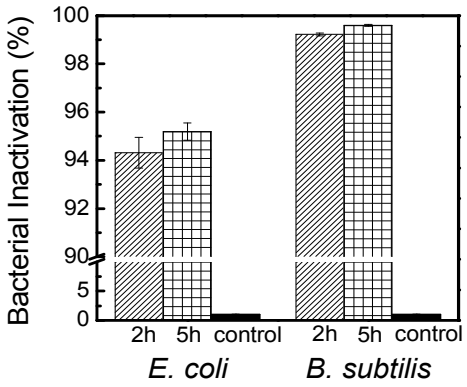

Fig. 5 Short term exposures of bacterial cells to sonochemically grown ZnO nanorods.

Our anti-microbial results for *E. coli* were further compared with the results from other studies with different ZnO nanomaterials and ZnO nanorods prepared through different methods (sonochemistry, hydrothermal, and sol-gel combustion) (**Fig. 6**). We selected *E. coli* for this comparison, since this microorganism is commonly used in anti-microbial investigations with ZnO nanomaterials. The results show that our method resulted in much higher microbial inactivation than most commercially produced ZnO nanomaterials. Furthermore, our sonochemical method of synthesis generated slightly higher anti-microbial properties than other sonochemical methods.

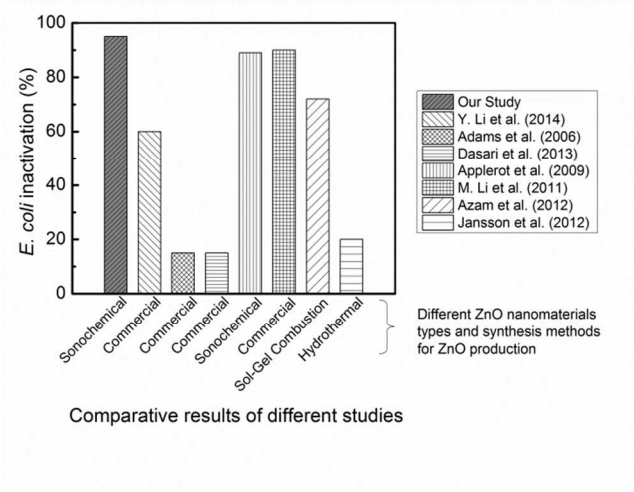

Fig. 6 Comparative results of ZnO nanomaterials antibacterial activity against *E. coli*. In this graph, the percent *E. coli* inactivation of ZnO in our study was compared with other studies [11, 26, 27, 39-42].

The long-term investigation of cell growth inhibition on the ZnO coated and uncoated surfaces were also investigated. **Fig. 7** shows the SEM images of glass slides with and without ZnO nanorods after microbial growth for 48 h in Tryptic Soy Broth (TSB). The results show that the glass slides containing ZnO nanorods inhibited biofilm formation, as opposed to uncoated glass slides. Clearly, the ZnO coated glass surfaces created an unfavourable environment for biofilm formation. These results suggest that coated surfaces with ZnO can inhibit microbial growth and prevent biofilm formation.

3.5. Mechanisms of toxicity of ZnO nanorods

Previous studies have suggested that the microbial inactivation by ZnO nanostructures could potentially be caused by the generation of reactive oxygen species (ROS), notably H_2O_2.

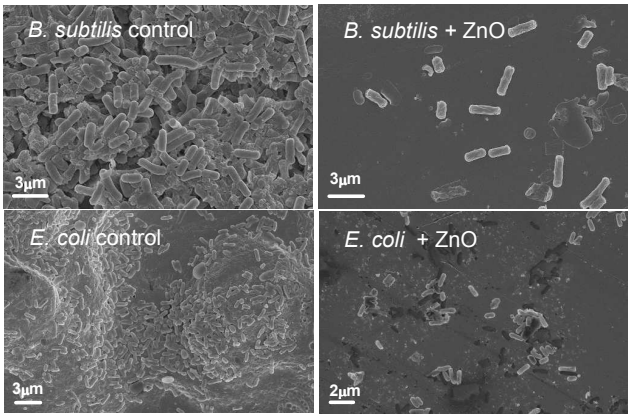

Fig. 7 Biofilm formations on glass substrates with and without ZnO nanorods

The produced ROS molecules can damage cell membranes and eventually cause cell death.[43] Oxidative stress by ROS has also been described to be responsible for microbial inactivation by several nanomaterials.[26, 44, 45] Since ZnO nanorods were found to be toxic to bacterial cells in this study, the GSH oxidation assay was employed to understand the toxicity mechanism of ZnO nanorods. GSH is an intracellular antioxidant molecule found in bacteria and diverse organisms. GSH has thiol groups that get converted to glutathione disulfide in the presence of reactive oxygen species, such as H_2O_2. This unique property of GSH makes it suitable for the investigation of ROS production.[44] The results of the comparison of GSH loss with different ZnO concentrations is shown in **Fig. 8**.

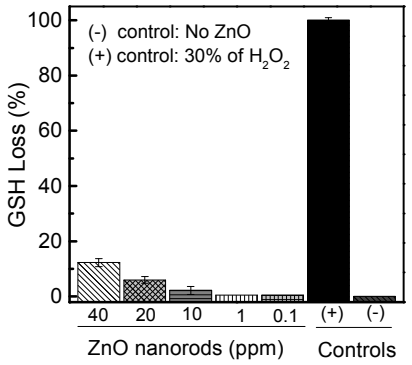

Fig.8 GSH loss results in the presence of different concentrations of ZnO nanorods suspensions.

In this study, the concentration of ZnO coating the slide was determined to be 21±3 ppm/cm^2. Therefore, the maximum concentration of ZnO nanorods that could detach from the slide during incubation would be 21±3 ppm. Hence, the concentrations of ZnO nanorods used in this study were 0.1, 1, 10 and 20 ppm to take into consideration a range of ZnO concentrations that could detach from the slide, as well as the maximum possible ZnO concentration that could be released from the coated surfaces. The 40 ppm concentration was also included in the experiments to investigate the H_2O_2 trend with increasing concentrations of ZnO nanorods. In the assay, the GSH loss (%) was calculated to indicate H_2O_2 production. H_2O_2 was used as a positive control, while the negative control was sodium bicarbonate. As seen in **Fig. 8**, statistically significant GSH loss occurred in the positive control above 20 ppm and no GSH loss was observed in the negative control. The results also showed that increasing concentrations of the ZnO nanorods led to increasing loss of GSH. These results suggest that ZnO nanorods can produce ROS, such as H_2O_2 and that its toxicity is concentration dependent.

Another potential ROS produced by nanomaterials is superoxide anion ($O_2^{\bullet-}$). The production of this oxygen species can be investigated using the XTT reduction assay. In this assay, TiO_2 was used as a positive control since this nanomaterial is well known to produce superoxide anions.[44] The results demonstrated that sonochemically grown ZnO nanorods did not produce superoxide anion even at high concentrations of ZnO nanorods and long exposure times (**Fig. S1**†).

Penetration of ZnO nanostructures through the bacterial cell wall, as well as the release of Zn^{2+} ions from dissolution of ZnO were also proposed as possible mechanisms for the antibacterial activity of ZnO.[13, 46] In the present study, we investigated the release of Zn^{2+} ions (see SI †) by employing atomic absorption spectroscopy. The results show that the glass slides coated with ZnO nanorods released 1.56±0.22 ppm Zn^{2+} ions per cm^2 of glass surface during the 5 h incubation period (**Table-S1**†).

Zinc ion concentrations below 5 ppm are considered to be safe by the EPA[47], additionally plate count assays of cells exposed to Zn^{2+} (see SI †) presented no cell death when the zinc ion concentrations were 10 ppm. Hence, the release of Zn^{2+} ions was disregarded as a possible mechanism of toxicity for ZnO nanorods.

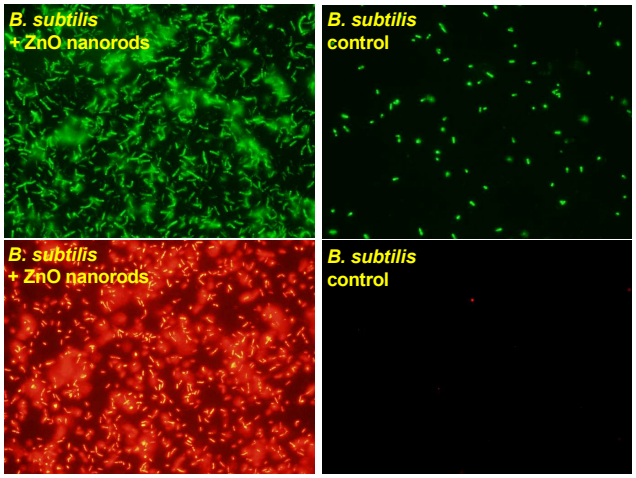

Fig.9 Representative images after cell staining of *Bacillus subtilis* through LIVE/DEAD assay on glass slides containing ZnO nanorods.

Another potential mechanism of anti-microbial property of ZnO nanorods could be the direct contact between bacterium and the nanorods on the surfaces. Bacterial cells tend to naturally deposit on surfaces during growth. After cell deposition membrane stress could occur due to the sharp edges of ZnO nanorods as seen in **Fig. 9**. This interaction between the nanorods and the cells could lead to cell membrane disruption and cell death. In the presence study, fluorescence microscopy images using the LIVE/DEAD staining in the presence or absence of nanorods show that the higher numbers of dead cells (red cells)

were observed on coated slides (**Fig. 9**.) However, in the control images, where there were no ZnO nanorods, little or no dead cells were observed.

Therefore, it can be concluded that the toxicity of ZnO nanorods is not the result of superoxide anion production or zinc ion released from nanorods. Instead, H_2O_2 production (**Fig. 8**) and membrane damage (**Fig. 9**) play an important role in the anti-microbial properties of ZnO nanorods. It is, however, possible that the antimicrobial properties of the ZnO nanorods can be the effect of other mechanisms not investigated in this study.

3.6. Cytotoxicity of ZnO nanorods

The application of ZnO as anti-microbial coatings have recently attracted attention for the biomedical sector.[23] The safety and human health effects of ZnO nanorods are, however, still not well established. Therefore, in the present study, we investigated the cytotoxicity of these ZnO nanorods to NIH 3T3 fibroblasts. The mammalian cell viability was represented as percent cell viability as shown in **Fig. 10**. The positive control contained benzalkonium chloride and the negative control had no ZnO nanorods. The results showed that the cytotoxicity increased with increasing concentrations of ZnO nanorods. If all the sonochemically grown ZnO nanorods were to detach from the coated surfaces, the maximum concentration of nanorods in the solution would be 21±3 ppm per 1 cm^2 glass surface. The cytotoxicity results show that 20 ppm ZnO nanorods present little or no cytotoxicity (**Fig. 10**).

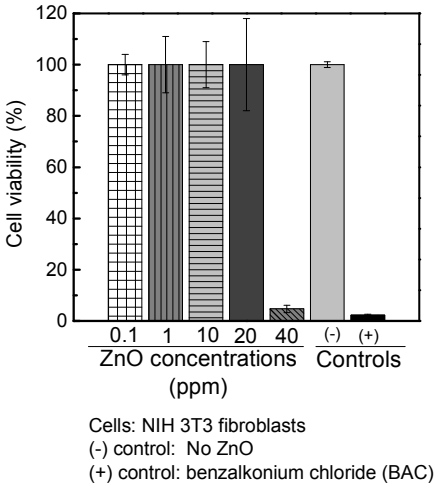

Fig. 10 Cytotoxicity results of different concentrations of ZnO nanorods against NIH 3T3 fibrolast cells.

Conclusion

This work reports the successful synthesis of ZnO nanorods using sonochemistry on glass surfaces. Raman and XPS studies revealed the formation of hexagonal (wurtzite) crystal structures of ZnO with a tensile stress on the Zn – O dative bond. SEM micrograph demonstrated homogenous coating with uniformly shaped nanostructures. The nanomaterial was found to inactivate over 90% of the microorganisms in the first 2 h. Gram-positive bacteria were, however, more sensitive to ZnO nanorods than Gram-negatives. The potential mechanisms of bacterial toxicity were attributed to H_2O_2 production and cell membrane damage. ZnO nanorods coating was also found to prevent biofilm formation. In the case of mammalian cell toxicity, the concentration used to coat the slides was shown to be non-toxic to fibroblast cells.

The results of the study suggest that sonochemical route for antimicrobial coatings are fast, cost effective alternative to other growth methods, which usually require extreme vacuum, temperature or time. Since ultrasound technology is already used in industry, the application of the sonochemical growth technique show great promise for large scale manufacturing of antimicrobial coatings for medical devices, medical implants and textile industry.

Acknowledgements

We thank the Turkish Ministry of National Education for supporting Tugba Onal Okyay with a Graduate Research Fellowship. We would like to thank Ralp B. Arlinghaus (Hubert L. Stringer Chair of Cancer research, MD Anderson Cancer Center, Houston Texas) for providing NIH 3T3 fibroblast cells and Dr. Enver Tarhan (Izmir Institute of Technology, Physics Department, Izmir Turkey) for the Raman Spectroscopy analysis.

Notes and references

[a] *Department of Civil and Environmental Engineering. University of Houston, Houston, TX-77004, USA. Fax: 713-743-4260; Tel: 713-743-1495; E-mail: dfrigirodrigues@uh.edu*

[b] *Department of Electrical and Electronics Engineering. Gediz University,35660 Izmir, Turkey. Fax: +90(232)355 0046; Tel:+90(232)355 0000; E-mail: yavuz.bayam@gediz.edu.tr*

† Electronic Supplementary Information (ESI) available: [Method for the XTT reduction assay, the result of XTT reduction assay, the determination of zinc ions, zinc ion concentrations released from glass slides, zinc ion concentrations in different ZnO nanorods suspensions, plate count method to test the toxicity of zinc ions, and plate count results.]. See DOI: 10.1039/b000000x/

1 A. Name, B. Name and C. Name, *Journal Title*, 2000, **35**, 3523; A. Name, B. Name and C. Name, *Journal Title*, 2000, **35**, 3523.

1. S. E. McNeil, *Journal of Leukocyte Biology*, 2005, **78**, 585.
2. O. Lupan, L. Chow, G. Chai, L. Chernyak, O. Lopatiuk-Tirpak and H. Heinrich, *physica status solidi (a)*, 2008, **205**, 2673-2678.
3. C. Shoou-Jinn, H. Ting-Jen, I. C. Chen and H. Bohr-Ran, *Nanotechnology*, 2008, **19**, 175502.
4. A. Fulati, S. M. U. Ali, M. H. Asif, N. u. H. Alvi, M. Willander, C. Brännmark, P. Strålfors, S. I. Börjesson, F. Elinder and B. Danielsson, *Sensors and Actuators B: Chemical*, 2010, **150**, 673-680.
5. L. Liao, H. B. Lu, M. Shuai, J. C. Li, Y. L. Liu, C. Liu, Z. X. Shen and T. Yu, *Nanotechnology*, 2008, **19**, 175501.
6. A. Menzel, K. Subannajui, F. Güder, D. Moser, O. Paul and M. Zacharias, *Advanced Functional Materials*, 2011, **21**, 4342-4348.
7. S. M. Al-Hilli, M. Willander, A. Öst and P. Strålfors, *Journal of Applied Physics*, 2007, **102**, -.

8. K. a. A. Chitra, G., *International Food Research Journal*, 2013, **20**, 59-64.
9. A. Toolabi, Zare, M. R., Rahmani, A., Hoseinzadeh, E., Sarkhosh, M. and Zare, M., *J. Basic. Appl. Sci. Res.*, 2013, **3**, 221-226.
10. F. Arabi, Imandar, M., Negahdary, M., Imandar, M., Noughabi, M.T., Akbari-dastjerdi, H. and Fazilati, M., *Annals of Biological Research* 2012, **3**, 3679-3685.
11. T. Jansson, Z. J. Clare-Salzler, T. D. Zaveri, S. Mehta, N. V. Dolgova, B.-H. Chu, F. Ren and B. G. Keselowsky, *Journal of Nanoscience and Nanotechnology*, 2012, **12**, 7132-7138.
12. R. S. Subhasree, D. Selvakumar and N. S. Kumar, *Letters in Applied NanoBioScience*, 2012, **1**, 2-7.
13. M. Jaisai, Baruah, S., and Dutta, J. , *Journal of Nanotechnol.*, 2012, **3**, 684–691.
14. J. J. Wu, Wen, H. I., Tseng, C. H., Liu, S. C. , *Adv. Funct. Mater*, 2004, **14**, 806–810.
15. Y. W. Heo, Varadarajan, V., Kaufman, M., Kim, K., Norton, D. P., Ren, F., Fleming, P. H., *Appl.Phys. Lett.* , 2002, **81**, 3046–3048.
16. Z. L. Wang, *Advance materials*, 2003, **15**, 5.
17. H. Yuan, Zhang, Y. and *J. Cryst. Growth*, 2004, **263**, 119–124.
18. Y. Sun, Fuge, G. M., Ashfold, M. N. R., *Chem. Phys. Lett*, 2004, **396**, 21–26.
19. D. Polsongkram, P. Chamninok S. Pukird L. Chow, O. Lupan and H. K. G. Chai , S. Park , A. Schulte *physica B*, 2008, **403**, 3713-3717.
20. S.-H. Jung, Oh, E., Lee, K-H., Jeong, S-H., Yang, Y. and Park, C. G. , *Bulletin of the Korean Chemical Society*, 2007, **28**, 1457.
21. P. K. Vabbina, Nayyar, P., Nayak, A. P., Katzenmeyer, A.M., Logeeswaran V.J., Pala, N., Saif Islam, M. and Talin A.A. , *Proc. of SPIE* 2010, **8106 81060H-1.**
22. J. J. Dong, Zhen, C. Y., Hao, H. Y., Xing, J., Zhang, Z. L., ZhengZ.Y. and Zhang,W. Z., *Nanoscale research letters*, 2013, **8**, 378.
23. I. E. Mejias Carpio, C. M. Santos, X. Wei and D. F. Rodrigues, *Nanoscale*, 2012, **4**, 4746-4756.
24. J. Fan, T. Onal Okyay and D. Frigi Rodrigues, *Journal of Hazardous Materials*, 2014, **279**, 236-243.
25. T. Onal Okyay and D. Frigi Rodrigues, *Ecological Engineering*, 2014, **62**, 168-174.
26. Y. Li, J. Niu, W. Zhang, L. Zhang and E. Shang, *Langmuir*, 2014, **30**, 2852-2862.
27. T. P. Dasari, K. Pathakoti and H.-M. Hwang, *Journal of Environmental Sciences*, 2013, **25**, 882-888.
28. F. Ahmed and D. F. Rodrigues, *Journal of Hazardous Materials*, 2013, **256–257**, 33-39.
29. P. K. Samanta, Patra, S. K., Ghosh, A. and Chaudhuri, P. R. , *International Journal of NanoScience and Nanotechnology*, 2009, **1**, 81-90.
30. I. Calizo, Alim, K. A., Fonoberov, V. A., Krishnakumar, S., Shamsa, M., Balandin, A. A. and Kurtz, R., *Proc. of SPIE*, 2007, **6481**, 1-8.
31. S. M. Soosen, J. Koshy, A. Chandran and K. C. George, *Indian Journal of Pure & Applied Physics*, 2010, **48**, 703-708.
32. C. D. Wagner, W. M. Riggs, L. E. Davis and J. F. Moulder, *Handbook of X-ray Photoelectron Spectroscopy*, 1st edn., Perkin-Elmer Corporation, Minnesota, USA, 1979.
33. P. Gangopadhyay, R. Kesavamoorthy, S. Bera, P. Magudapathy, K. G. M. Nair, B. K. Panigrahi and S. V. Narasimhan, *Physical Review Letters*, 2005, **94**, 047403.
34. K. Luo, T. P. St. Clair, X. Lai and D. W. Goodman, *The Journal of Physical Chemistry B*, 1999, **104**, 3050-3057.
35. H.-B. Fan, X.-L. Zheng, S.-C. Wu, Z.-G. Liu and H.-B. Yao, *Chinese Physics B*, 2012, **21**, 038101.
36. R. S. Subhasree, Selvakumar, D., Kumar, N. S. , *Letters in Applied Nano-bio science*, 2012, **1**.
37. D. F. Rodrigues and M. Elimelech, *Environmental Science & Technology*, 2010, **44**, 4583-4589.
38. F. Ahmed, C. M. Santos, J. Mangadlao, R. Advincula and D. F. Rodrigues, *Water Research*, 2013, **47**, 3966-3975.
39. L. K. Adams, D. Y. Lyon and P. J. J. Alvarez, *Water Research*, 2006, **40**, 3527-3532.
40. G. Applerot, N. Perkas, G. Amirian, O. Girshevitz and A. Gedanken, *Applied Surface Science*, 2009, **256**, S3-S8.
41. M. Li, L. Zhu and D. Lin, *Environmental Science & Technology*, 2011, **45**, 1977-1983.
42. A. Azam, A. S. Ahmed, M. Oves, M. S. Khan, S. S. Habib and A. Memic, *International Journal of Nanomedicine*, 2012, **7**, 6003-6009.
43. K. Tam, Djurisic, A., Chan, C., Xi, Y., Tse, C., Leung, Y., Chan, W., Leung, F., Au, D. , *Thin Solid Films*, 2008, **516**, 6167-6174.
44. S. Liu, T. H. Zeng, M. Hofmann, E. Burcombe, J. Wei, R. Jiang, J. Kong and Y. Chen, *ACS Nano*, 2011, **5**, 6971-6980.
45. S. Kang, M. Herzberg, D. F. Rodrigues and M. Elimelech, *Langmuir*, 2008, **24**, 6409-6413.
46. T. Jansson, Clare-Salzler, Z.J., Zaveri, T. D., Mehta, S., Dolgova, N. V., Chu, B., Ren, F., and Kesolowsky, B. G. , *Journal of nanoscience and nanotech*, 2012, **12**, 7132-7138.
47. U. S. EPA, 2014.